Proc. Natl. Acad. Sci. USA
Vol. 93, pp. 828–833, January 1996
Cell Biology

In vivo examination of membrane protein localization and degradation with green fluorescent protein

RANDOLPH Y. HAMPTON*†, ANN KONING‡, ROBIN WRIGHT‡, AND JASPER RINE*

*Division of Genetics, Department of Molecular and Cell Biology, University of California, Berkeley, CA 94720; and ‡Department of Zoology, University of Washington, Seattle, WA 98195

Communicated by Randy Schekman, University of California, Berkeley, CA, August 14, 1995 (received for review June 9, 1995)

ABSTRACT **To test the utility of green fluorescent protein (GFP) as an *in vivo* reporter protein when fused to a membrane domain, we made a fusion protein between yeast hydroxymethylglutaryl–CoA reductase and GFP. Fusion proteins displayed spatial localization and regulated degradation consistent with the native hydroxymethylglutaryl–CoA reductase proteins. Thus, GFP should be useful in the study of both membrane protein localization and protein degradation *in vivo*.**

The green fluorescent protein (GFP) from jellyfish retains its ability to fluoresce *in vivo* when expressed in other organisms, including bacteria, *Caenorhabditis elegans*, and *Drosophila* (1–3). These studies indicated that GFP might have broad applications as a reporter function in the study of localization and turnover of membrane proteins. To test this idea, we have made fusion genes that join *Saccharomyces cerevisiae* hydroxy methylglutaryl–CoA reductase (HMG-R) and GFP. Like mammalian HMG-R, the yeast Hmg1p and Hmg2p isozymes are similarly restricted to the endoplasmic reticulum (ER) (ref. 4 and A.K. and R.W., unpublished data). Furthermore Hmg2p is subjected to regulated degradation in a manner strikingly similar to that of the mammalian enzyme (5–7). Since the N termini determine both localization and turnover, a fusion protein between the N-terminal region of Hmg2p and GFP was predicted to display both spatial and temporal regulation similar to that of the native Hmg2p. Our studies demonstrated that the GFP moiety could serve as an *in vivo* reporter of membrane protein spatial localization and half-life.

MATERIALS AND METHODS

Culture Media and Growth Conditions. Yeast strains were grown at 30°C in YM medium supplemented with glucose and appropriate amino acids as described (8).

DNA Techniques. Plasmid TU65 (2) was the source of the GFP coding region, and has an *Age* I site 13 bp 5′ to the GFP start codon (A CCG GTA GAA AAA) and an *Eco*RI site 3′ to the GFP stop codon. TU65 was digested with *Age* I, blunt-ended with Klenow fragment of DNA polymerase I, and then digested with *Eco*RI to yield a blunt/*Eco*RI fragment of ≈750 bp. This fragment was then inserted into pBluescript II KS (+) to give pRH402. The GFP coding region was excised from pRH402 by digestion with *Cla* I, treatment with the Klenow fragment of DNA polymerase I, and digestion with *Eco*RI. The resulting fragment was fused to *HMG2* by insertion into the internal *Bsa*BI site and the proximal *Eco*RI site of pRH144-2 (7). The fusion junction is located at nt 2009 (numbered from the start codon) of *HMG2* (Fig. 1). The 750-bp *Cla*I–*Eco*RI fragment from pRH402, with the *Eco*RI site blunt-ended was fused to the *HMG1* coding region by inserting this piece into the internal *Cla*I site and the *Bsa*BI of pRH105-25 to yield pRH408, with an in-frame fusion of the GFP coding region to nt 2106 (numbered from the start codon) of *HMG1*. The predicted fusion proteins have N-terminal transmembrane regions up to Asp-671 (Hmg2p) or Asp-702 (Hmg1p) fused to either seven or six, respectively, polylinker-encoded amino acids and then to GFP.

Yeast Strains and Growth. Yeast strain RWY60 (*his3Δ200 lys2-801 ade2-101 ura3-52 met pep4::hisG*) was transformed with *HMG-R::GFP* expression vector pRH407 (*HMG1::GFP*) or pRH408 (*HMG2::GFP*) as described (7). Each plasmid was introduced into the recipient strain by targeted integration at the *Stu* I site of the *ura3-52* allele. The resultant strains were named RHY404 (RWY60 with *GPDp-HMG1::GFP* integrated at *URA3*), RHY405 (same as RHY404 but with a double integrant, as confirmed by DNA blotting) and RHY406 (RWY60 with *GPDp-HMG2::GFP* integrated at *URA3*). The average fluorescence of the *HMG1::GFP* double integrant (as measured by flow cytometry) was similar to that of the average fluorescence of the *HMG2::GFP* single integrant.

Strains expressing the authentic *HMG2* (RHY183) or *HMG1* (RHY105-25) coding regions integrated into the genome and driven by the GPD promoter were constructed as described (8). The above two strains were used for the comparison of the GFP fusion-expressing strains with those expressing the native proteins in the electron microscopic studies of Fig. 4. Strain RHY420 (used in Fig. 5 *A*, *B*, and *D*) expressed the GPD-promoter driven *HMG2* gene from a plasmid integrated at the *URA3* locus as the only source of HMG-R activity and had a disruption of the *PEP4* gene.

Optical Methods. Microscopy was performed on a Nikon Optiphot microscope with epifluorescence illumination. GFP fluorescence was observed in living cells with a Nikon DM510 filter for fluorescein fluorescence with illumination at 390 nm and long-bandpass emission. 4′-6-diamidino-2-phenylindole (DAPI) fluorescence (for DNA) was observed with a Nikon DM400 filter with illumination at 365 nm and emission at >400 nm. *In vivo* DAPI staining was done by adding DAPI (final concentration of 1 μg/ml) to the growing cultures of cells 3 h prior to examination and then washing the cells extensively prior to examination. Fields were photographed with Kodak Ektachrome P1600 color reversal film and transferred to CD Image Process color labs (Berkeley, CA). Confocal laser scanning microscopy and R6 fluorochrome staining (Fig. 3) were performed by using equipment and parameters identical to those described (8, 9). The digitized images from the fluorescent and confocal experiments were prepared as graphics by using Adobe Photoshop ver 2.5.1 and Canvas ver 3.5 and

The publication costs of this article were defrayed in part by page charge payment. This article must therefore be hereby marked "*advertisement*" in accordance with 18 U.S.C. §1734 solely to indicate this fact.

Abbreviations: GFP, green fluorescent protein; ER, endoplasmic reticulum; HMG-R, hydroxymethylglutaryl–CoA reductase; DAPI, 4′-6-diamidino-2-phenylindole; GPD, glucose-6-phosphate dehydrogenase; $loop_{6\text{-}7}$ antigen, lumenal loop of Hmg2p between the putative 6th and 7th transmembrane regions.

†To whom reprint requests should be sent at present address: Department of Biology, University of California, San Diego, #0116, 9500 Gilman Drive, La Jolla CA, 92093-0116.

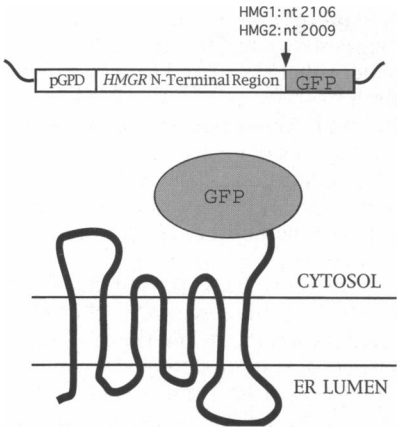

FIG. 1. Representations of the *HMG-R::GFP* fusion genes (*Upper*) and the HmgRp–GFP fusion proteins (*Lower*) produced from those genes. The arrow marks the site of each fusion junction with the nucleotide number of each HMG-R coding region, numbered from the start codon. Both fusion proteins were expressed from the strong, constitutive glucose-6-phosphate dehydrogenase (GPD) promoter. The HmgR portion of the fusion included the entire membrane domain, the linker region, and a small portion of the catalytic domain. The *HMG1* junction point was at a *Cla* I restriction site in the *HMG1* coding region, and the *HMG2* junction point was at a *Bsa*BI site in the *HMG2* coding region.

printed on a Kodak PrintEase ES printer (Figs. 2 and 5*C*) or a Tektronix PhaserIISDX dye sublimation printer.

Flow Cytometric Analysis. Living cells were analyzed by flow microfluorimetry by using a FACSscan (Beckton Dickinson) analytical flow microfluorimeter with settings typically employed for fluorescein-labeled antibody analysis. Histograms shown in Fig. 5*B* each represented at least 9000 cells.

Electron Microscopy. Cells were grown to log phase (1 OD_{600}/ml) in YM glucose medium supplemented with the appropriate amino acids and 2% casamino acids and prepared for electron microscopy as previously described (10) with some modifications. Specifically, 40 ml of the culture was rapidly fixed with 10 ml of 5× phosphate-buffered fixative [1× = 137 mM NaCl/2.7 mM KCl/1.5 mM KH_2PO_4/6.5 mM Na_2HPO_4/1 mM $CaCl_2$/1 mM $MgCl_2$/2% (vol/vol) glutaraldehyde, pH 7.4] for 5 min at room temperature. Cells were pelleted briefly, resuspended in 1× fixative, and fixed overnight at 4°C. After four washes with distilled water, cells were resuspended in 2 ml of distilled water and, 2 ml of 4% (wt/vol) potassium permanganate was added. After 5 min at room temperature, the cells were pelleted and incubated with 6 ml of fresh 2% (wt/vol) potassium permanganate for 1 h at room temperature. Finally, cells were stained *en bloc* with 1% uranyl acetate, dehydrated in a graded ethanol series, embedded in Pelco Ultra Low Viscosity Resin (Ted Pella, Redding, CA), sectioned, and stained as described (10).

Biochemical Analysis of Protein Stability. The half-life of the fusion protein was compared with that of native Hmg2p by analyzing immunoblots after protein synthesis was inhibited with cycloheximide at various times, as described (8). Regulated degradation of the Hmg2p–GFP fusion protein in living cells was studied by allowing cells to grow to stationary phase. Upon reaching stationary phase, Hmg2p continues to be degraded after cessation of protein synthesis, resulting in a drastically lowered immunoblotting signal when compared with the steady-state levels in logarithmic phase. The cells were grown in supplemented YM medium to late logarithmic phase ($OD_{600} \approx 0.9$). Aliquots from this stock were separated and, where indicated, were treated with lovastatin (final concentration of 25 μg/ml). At the same time, a fresh culture was inoculated at low density from the stock to provide a logarithmic-phase sample of cells at the end of the experiment. Cells were then allowed to resume growth at 30°C for 18 h, at which time equal numbers of cells were harvested and subjected to immunoblotting analysis as described (8).

Hmg2p and Hmg2p–GFP fusion protein were detected on immunoblots by using a polyclonal antibody raised against a fusion protein between the maltose binding protein (MBP) and the lumenal loop of Hmg2p between the putative 6th and 7th transmembrane regions ($loop_{6-7}$ antigen). The $loop_{6-7}$ antigen was made by PCR amplification of the region of the *HMG2* gene encoding the loop, in-frame fusion of the PCR product to the MBP coding region of the pMal vector (New England Biolabs, MA), and purification of the plasmid-expressed MBP–HMG2 $loop_{6-7}$ antigen fusion protein, as per the manufacturer's instructions.

RESULTS AND DISCUSSION

Distribution of HmgRp–GFP in Living Yeast. Strains expressing either the Hmg1p–GFP (Fig. 2*A*) or the Hmg2p–GFP (Fig. 2*B*) fusions (RHY405 or RHY406, respectively), were examined by fluorescence microscopy. The nuclear DNA was stained *in vivo* with DAPI (1 μg/ml). Comparison of the fluorescence from the GFP fusion (Fig. 2 *Left*) with that from the DAPI-stained nuclear DNA (Fig. 2 *Right*) showed that both proteins were localized in the nuclear envelope, as expected (red arrows). This pattern is especially prevalent in the Hmg1p–GFP-expressing cells. In addition to the perinu-

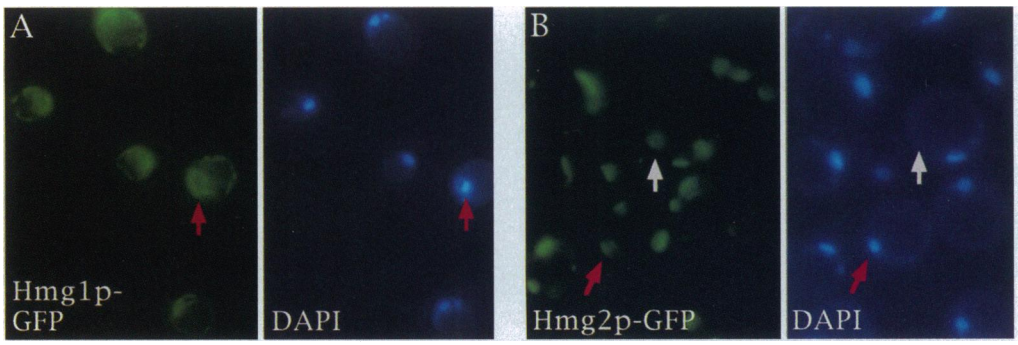

FIG. 2. Yeast strains expressing the *HMGR::GFP* fusion genes. Strains expressing either the *HMG1::GFP* fusion gene (RHY405) (*A*) or the *HMG2::GFP* fusion gene (RHY406) (*B*) were grown in supplemented YM medium. Three hours before the cells were harvested, the nuclear stain DAPI was introduced into the cultures at a final concentration of 1 μg/ml. The cells were harvested at $OD_{600} \approx 0.5$, washed, and examined for GFP fluorescence (*Left*) or DAPI fluorescence (*Right*), as described. Red arrows indicate sites of GFP perinuclear fluorescence, and the white arrow in *B* indicates a site of one of the bright extranuclear patches present in cells expressing Hmg2p–GFP. The images were made by transferring color-slide micrographs to CD-ROM, with subsequent layout and printing as described in *Materials and Methods.* The sizes of the cells in *B* appear larger because the image is an enlargement of a smaller portion of the microscopic field than that used for *A*. The actual sizes of the cells were the same.

clear staining, cells expressing the Hmg1p–GFP fusion show a reticular fluorescence pattern in the cytoplasm and cell periphery which is typical of ER-localized proteins in yeast (11, 12). The Hmg2p–GFP fusion was present in one or more patches at the cell periphery or near the nucleus (white arrow). In this figure, the Hmg1p–GFP-expressing strain (RHY405) had a double integrant of the expression plasmid and thus exhibited more intense fluorescence than the same strain with a single integration. However, the distribution of Hmg1p–GFP fluorescence in the single-integrant strain (RHY404) was identical to the distribution in the double integrant (data not shown). The double integrant of the *HMG1::GFP* reporter was used in this comparison because the level of fluorescence between this strain and that of the *HMG2::GFP* single integrant was almost identical as measured by flow cytometry (data not shown).

Laser scanning confocal microscopy (Fig. 3*A*) demonstrated that Hmg2p–GFP was also distributed in the cell in a manner consistent with the characteristic ER localization, such that each cell had light perinuclear fluorescence (solid arrow) as well as peripheral staining (open arrow). As in the lower resolution images shown in Fig. 2*B*, bright patches of staining were also visible, either associated with the perinuclear ring or separate from it.

Hmg2–GFP and Membrane Proliferations. The bright patches of staining seen at the light microscopic level appeared to be sites of proliferation of the ER membrane, similar to those described (4). To test this idea, we examined the cells with two additional methods: *in vivo* fluorescent dye staining and electron microscopy.

The strain expressing the Hmg2–GFP fusion (RHY406) was stained with R6 (red fluorescence), which labels areas of membrane proliferation (8, 9), and the cells were examined by confocal microscopy at filter settings for either GFP fluorescence (Fig. 3*B Upper*) or R6 fluorescence (Fig. 3*B Lower*). In all cells examined, the GFP staining overlapped with the R6 staining, indicating that the structures that contained Hmg2p–GFP had the biophysical properties of membranes undergoing proliferation. GFP alone did not give a signal with the R6 settings.

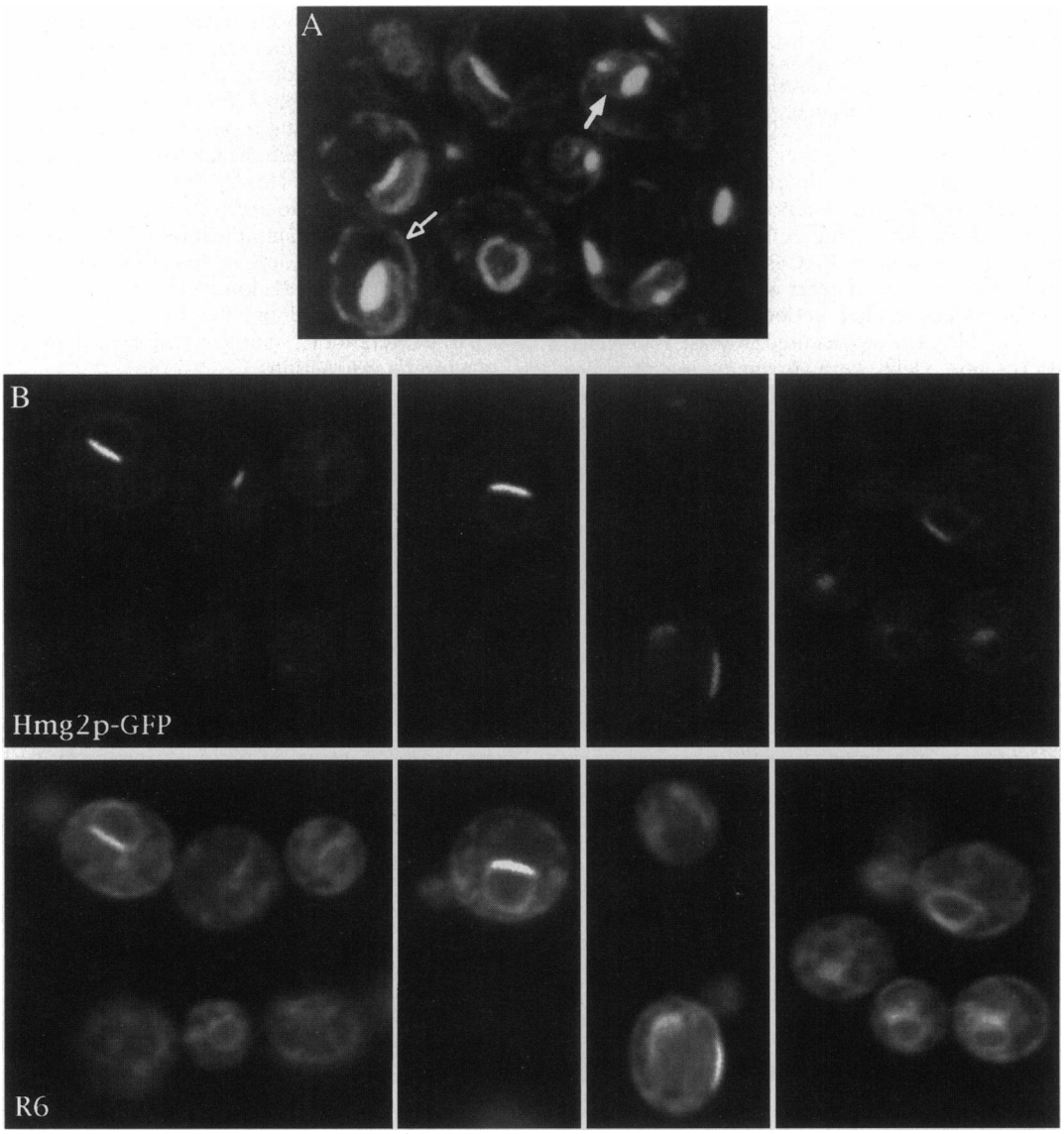

FIG. 3. Confocal image of Hmg2p–GFP fluorescence. (*A*) Cells harboring the *HMG2::GFP* reporter gene (RHY406) were examined directly without fixation by confocal microscopy as described. The image shown represents the central 2.5 μm of the cell (5 of 15 central optical sections). The open arrow indicates an example of peripheral fluorescence, and the solid arrow points to an example of perinuclear fluorescence, both of which are typical of ER proteins. (*B*) Simultaneous examination of Hmg2p–GFP fluorescence and R6 fluorescence. The same strain as in *A* was stained with R6 to label membrane sites of proliferation. Fields of cells were then examined by confocal microscopy by using filters for GFP fluorescence (*Upper*) or R6 fluorescence (*Lower*). (Bar = 5 μm.)

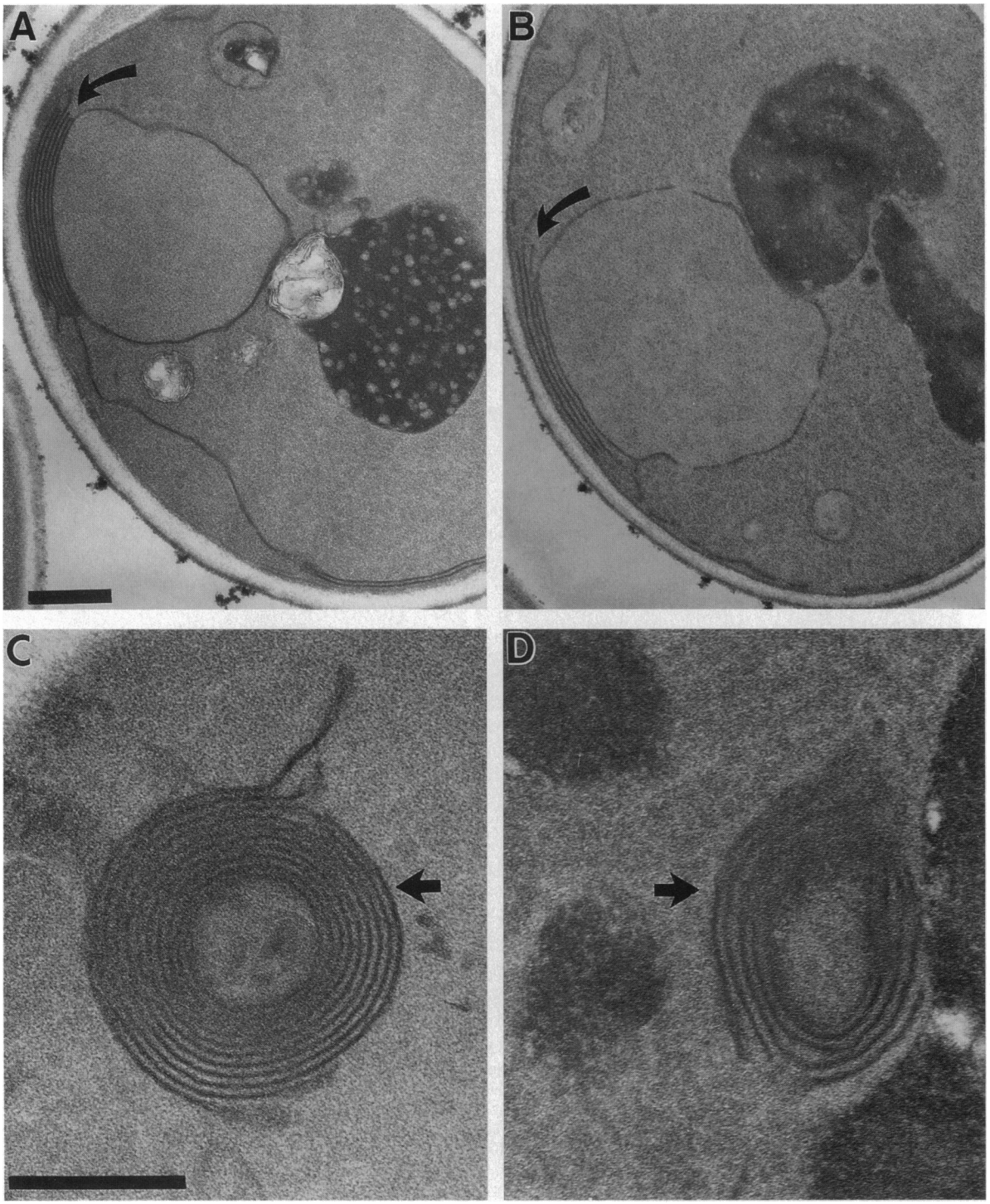

FIG. 4. Electron microscopy of isogenic strains expressing high levels of Hmg2p (RHY432) or Hmg2p–GFP (RHY406). (*A* and *C*) Membrane proliferations (arrows) seen in cells with the Hmg2p construct. (*B* and *D*) Membrane proliferations (arrows) seen in cells with the Hmg2p–GFP fusion. n, Nucleus; v, vacuole. (Bars = 500 nm.)

We next examined the ultrastructure of isogenic strains expressing either native Hmg2p (Fig. 4 *A* and *C*) or Hmg2p–GFP (Fig. 4 *B* and *D*) from identical promoters. In both strains, the predominant structures were strips of stacked membranes (Fig. 4 *A* and *B*), sometimes along the nuclear border, and concentric whorls of membrane separate from the nucleus (Fig. 4 *C* and *D*). Although the distance between the membrane layers in the Hmg2p–GFP-expressing strain appeared to be greater than those induced by native Hmg2p, the fusion protein caused the same types of proliferated structures as the native protein, and these structures were consistent with those visible *in vivo* by fluorescence microscopy.

In these strains, the expression of neither Hmg1p–GFP nor the native Hmg1p caused proliferations. This result was surprising since high levels of Hmg1p expression are known to induce karmellae (4). However, they demonstrated that the GFP fluorescence faithfully reported proliferations when and only when they were present.

Degradation of the Hmg2–GFP Fusion Protein. The Hmg2p protein is subject to regulated degradation at or in the ER itself (7). As in mammalian cells, the degradation of Hmg2p is regulated by the mevalonate pathway, such that high pathway flux causes a high degradation rate, and low flux causes a low

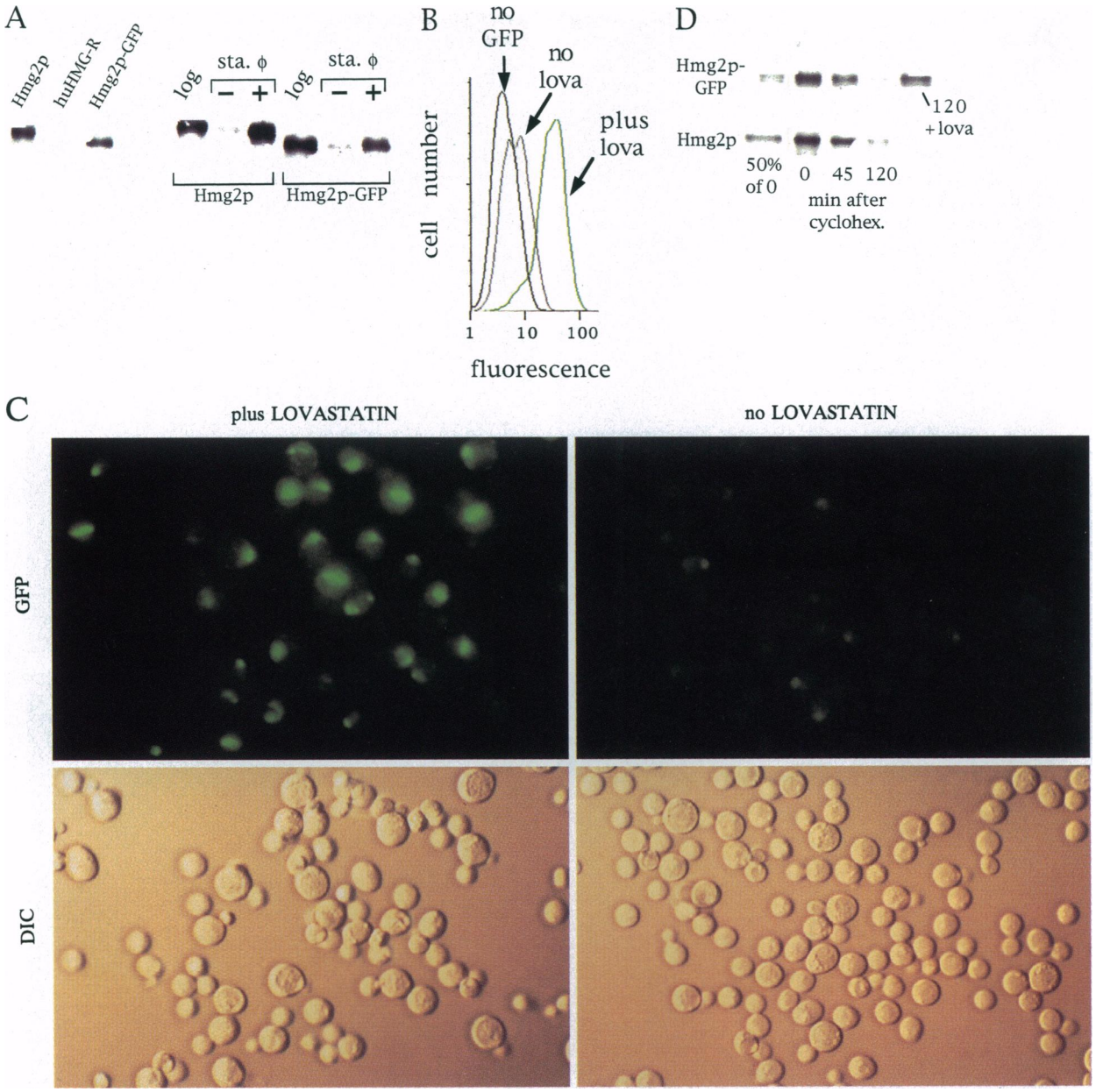

FIG. 5. Regulated degradation of the Hmg2p–GFP protein measured by biochemical (*A* and *D*) or optical (*B* and *C*) means. (*A*) Demonstration of the specificity of anti-Hmg2p $loop_{6\text{-}7}$ antiserum. The three lanes on the left show immunoblots of strains expressing native Hmg2p, human HMG-R (huHMG-R), or Hmg2p–GFP. The bands are appropriate sizes from the predicted coding regions, and the huHMG-R, which runs in the same region of the blot, was not detected. (*Right*) Strains expressing native Hmg2p (RHY420) or Hmg2p–GFP (RHY406) were grown to late logarithmic phase ($OD_{600} \approx 0.9$). From this stock, parallel cultures were grown to stationary phase (sta ϕ) in the absence (−) or presence (+) of 25 μg of lovastatin per ml for 18 h at 30°C. The stock cultures were also diluted into fresh medium to provide a logarithmic phase (log) culture of each strain. For each strain, lysates from equivalent numbers of cells from the log; sta ϕ, −; and sta ϕ, + were prepared and analyzed by immunoblotting with anti-Hmg2p $loop_{6\text{-}7}$ antigen. Each lane had ≈ 0.2 OD_{600} equivalents of cell lysate. (*B*) The strain expressing Hmg2p–GFP (RHY406) was grown to stationary phase in the presence (plus lova) or absence (no lova) of 25 μg of lovastatin per ml. Outgrowth was for 12 h at 30°C after late logarithmic phase ($OD_{600} \approx 0.9$). Cells were then analyzed by flow cytometry. An isogenic control strain expressing similar levels of Hmg2p was also tested in parallel (no GFP). (*C*) Cells from the flow cytometry experiment were also examined and photographed by fluorescence microscopy (*Upper*) or Nomarski [differential interference contrast (DIC)] optics (*Lower*). Cells grown to stationary phase in lovastatin are on the left side, and those grown in the absence of the drug are on the right side. (*D*) Estimation of protein half-life by immunoblotting after inhibition of protein synthesis with cycloheximide. Cultures of cells expressing either Hmg2p–GFP or Hmg2p at similar levels were grown to early logarithmic phase, placed in fresh medium, treated with cycloheximide, and incubated at 30°C as described (8). At the indicated times, aliquots were removed and prepared for immunoblotting with the anti-Hmg2p $loop_{6\text{-}7}$ antigen antiserum. The left lane in each row is the result of loading one-half of the amount of lysate used in the 0 min lane to show the signal that would result from 50% degradation of the initial immunoreactivity. A sample of the Hmg2p–GFP experimental culture was treated with 25 μg of lovastatin per ml immediately after the addition of cycloheximide and then allowed to incubate for 120 min to evaluate regulation of Hmg2p–GFP degradation (top row, right lane; 120 + lova).

degradation rate (5–7). The degradation of both Hmg2p–GFP and authentic Hmg2p was studied by using an antibody that recognizes a common Hmg2p-specific region, the lumenal loop between transmembrane domains 6 and 7 (Fig. 5*A*).

When a logarithmic-phase strain expressing the Hmg2p protein from the GPD promoter (RHY420) was grown to stationary phase, the degradation of Hmg2p continued after protein synthesis ceases, and the total Hmg2p immunoreac-

tivity declined drastically (Fig. 5*A*, lanes marked Hmg2p). The lane labeled log measured the steady-state amount of Hmg2p in a logarithmic-phase culture. When cultures were allowed to grow to stationary phase without lovastatin the amount of Hmg2p was much lower. If the mevalonate pathway were slowed by the inclusion of a small dose of lovastatin in the cultures during growth into stationary phase, the expected slowing of Hmg2p degradation occurred, and the loss of total immunoreactivity was prevented. The stable Hmg1p protein is not lost upon growth into stationary phase (data not shown). Thus, as in the other assays of Hmg2p regulated degradation (8), the loss of Hmg2p by growth into stationary phase was specific for the rapidly degraded isozyme and was regulated by the mevalonate pathway. The Hmg2p–GFP fusion protein also showed regulated degradation like the parent Hmg2p isozyme (Fig. 5*A*, lanes marked Hmg2p–GFP).

The fluorescence of the Hmg2p–GFP fusion was also subjected to regulated degradation, as measured by flow cytometry (Fig. 5*B*) and by examination of the cells by fluorescence microscopy (Fig. 5*D*). In this experiment, cells expressing the Hmg2p–GFP fusion were grown to stationary phase in the presence or absence of 25 μg of lovastatin per ml and examined by each technique. A non-GFP-expressing control was included in the histograms.

Both Hmg2p–GP and the Hmg2p were degraded at similar rates, with half-lives on the order of 1.5 h under these conditions. This was determined by inhibiting protein synthesis with cycloheximide and immunoblotting at various times (Fig. 5*D*). The loss of Hmg2p–GFP was prevented by addition of lovastatin (25 μg/ml) to a sample of the cycloheximide-treated culture at the beginning of the experiment. Taken together, these studies indicate that GFP will be a useful reporter for studying processive protein degradation as well as localization.

The authors thank Max Krummel and James Allison for the use of and assistance with the FACSscan analyzer, Don Rio and Tom Cline for use of Kodak Printers. R.Y.H. also wishes to thank Dago Dimster-Denk for instruction in classical mechanics and hydrocarbon coatings. This work was supported by grants from the Helen Hay Whitney Foundation and the California Chapter of the American Heart Association (R.Y.H.), the National Institutes of Health (GM35827 to J.R., GM45726 to R.W., and Training Grant T32GM07270), and by a Mutagenesis Center Grant from the National Institute of Environmental Health Sciences (P30ES01896-12).

1. Cody, C. W., Prasher, D. C., Westler, W. M., Prendergast, F. G. & Ward, W. W. (1993) *Biochemistry* **32,** 1212–1218.
2. Chalfie, M., Tu, Y., Euskirchen, G., Ward, W. W. & Prasher, D. C. (1994) *Science* **263,** 802–805.
3. Wang, S. & Hazelrigg, T. (1994) *Nature (London)* **369,** 400–403.
4. Wright, R., Basson, M., D'Ari, L. & Rine, J. (1988) *J. Cell Biol.* **107,** 101–114.
5. Edwards, P. A., Lan, S. F. & Fogelman, A. M. (1983) *J. Biol. Chem.* **258,** 10219–1222.
6. Chun, K. T., Bar, N. S. & Simoni, R. D. (1990) *J. Biol. Chem.* **265,** 22004–22010.
7. Hampton, R. Y. & Rine, J. (1994) *J. Cell Biol.* **125,** 299–312.
8. Koning, A. J., Lum, P. Y., Williams, J. M. & Wright, R. (1993) *Cell Motil. Cytoskel.* **25,** 111–128.
9. Terasaki, M. (1989) *Methods Cell Biol.* **29,** 125–135.
10. Wright, R. & Rine, J. (1989) *Methods Cell Biol.* **31,** 473–512.
11. Rose, M. D., Misra, L. M. & Vogel, J. P. (1989) *Cell* **57,** 1211–1221.
12. Preuss, D., Mulholland, J., Kaiser, C. A., Orlean, P., Albright, C., Rose, M. D., Robbins, P. W. & Botstein, D. (1991) *Yeast* **7,** 891–911.